Materials Research. 2017; 20(6): 1492-1502
DOI: http://dx.doi.org/10.1590/1980-5373-MR-2016-0772

Potency of $ZnFe_2O_4$ Nanoparticles as Corrosion Inhibitor for Stainless Steel; the Pigment Extract Study

Sadegh Mahvidi[a,b], Mehrnaz Gharagozlou[a]*, Mohammad Mahdavian[b], Sanaz Naghibi[c]

[a]Department of Nanomaterials and Nanocoatings, Institute for Color Science and Technology, P.O. Box: 1668814811, Tehran, Iran.
[b]Surface Coatings and Corrosion Department, Institute for Color Science & Technology, P.O. Box: 1668814811, Tehran, Iran.
[c]Young Researchers and Elite Club, Shahreza Branch, Islamic Azad University, Po. Box 311-86145, Shahreza, Iran.

Received: October 16, 2016; Revised: June 22, 2017; Accepted: July 27, 2017

The corrosion inhibition of nanoparticulates zinc ferrite (NZF) pigment was studied. The steel samples were immersed in the NZF pigment extract in 3.5 wt. % NaCl. Electrochemical tests such as electrochemical impedance spectroscopy (EIS) and polarization as well as surface analysis were employed to evaluate the effect of NZF on the steel corrosion. The concentration of Zn and Fe in the pigment extracts before and after immersion of mild steel samples was evaluated by inductively coupled plasma-optical emission spectrometry (ICP-OES). EIS results in total agreement with results of polarization test demonstrated superiority of NZF as an anticorrosion pigment. In the case of samples exposed to NZF extract, the higher resistance and lower double layer capacitance extracted from impedance spectra as well as lower current density from polarization results might be attributed to precipitation of an inhibitive layer on the surface. This was also supported by SEM/EDS and ICP-OES results.

Keywords: *Corrosion inhibitor, Zinc ferrite pigment, Pigment extract, EIS, ICP-OES.*

1. Introduction

Decades of academic research and industrial practice in organic coatings have led to the selection of a few pigments with excellent anticorrosive properties in a wide range of situations. Chromium-containing anticorrosion pigments have been extensively used for a long time. For instance, zinc chromate was one of the anticorrosive pigments most frequently used in the formulation of primers. Undoubtedly, they belong to the group of inhibitors, which exhibit excellent corrosion inhibitive performance. Unfortunately, chromium (VI) is carcinogenic and toxic; hence, the use of the chromium products is restricted and prohibited strictly[1-7]. It is important to bear in mind of the high anticorrosive action of entire coating system and environmental-friendly behavior at the same time[5,8-10]. Furthermore, the corrosion inhibition properties of numerous compounds have been examined through the years in the hope of providing an effective replacement[11-18]. By 2006, among the new nontoxic anticorrosive pigments, which were introduced as substitutes for traditional pigments, zinc phosphate has probably been the most widely accepted and it was incorporated in many paint formulations[3,7]. The toxicity level of this compound is 50 time less than chromates[1,5,19,20]. Although zinc phosphate gives good results, in certain cases, it is proved to have lower corrosion inhibition than zinc chromate[17,21]. Many attempts have been made to modify zinc phosphate to obtain a better alternative for zinc chromate[22,23].

Ferrites are acquiring increasing importance as alternative products. These inhibitive substances have not been studied as deeply as phosphates; but, in many accelerated tests they exhibit better performance than zinc phosphate[24]. Ferrites have a spinel structure with the general formula of $X.Fe_2O_3$ (X = MgO, ZnO or CaO). Ferrites can act as an inhibitive pigment and/or have barrier properties[25]. El-Ghaffar et. al are reported that the formation of a passive layer on the steel surface in the presence of zinc ferrite may be the result of pH control of the medium due to the hydrolysis of ferrite. They showed that the role of these pigments in protection is referred to the creation of an alkaline environment at the coating/metal interface via cation solubility. This phenomenon causes to form metal soaps as the passive layer[26].

As a prominent member of ferrite pigments zinc ferrite ($ZnFe_2O_4$) has attracted significant research interest because of its nontoxic nature and unique physical, mechanical and corrosion inhibition properties[27-30]. Meanwhile, several limitations and defects have been reported for conventional

*e-mail: gharagozlou@icrc.ac.ir

micron sized pigments[31]. To subdue disadvantages and to further improving the performance, using nanosized pigments is a recent practice. Due to their small particle size, nanomaterials exhibit special properties in different forms such as thin coatings.

The objective of this investigation was to study the inhibitive properties of NZF pigments in solution phase. The NZF pigment was synthesized under definite conditions and its anticorrosive properties was investigated by means of electrochemical techniques such as EIS and polarization of steel samples immersed in the pigment extracts in 3.5 wt. % NaCl aqueous solution. Moreover, the solubility of NZF pigments was evaluated by ICP-OES. In addition, composition and morphology of the precipitated layer on steel samples were studied by using scanning electron microscopy (SEM) and energy dispersive X-ray analysis (EDX) techniques.

2. Experimental

2.1 Low carbon steel panels

Composition of steel panels used for surface analysis and electrochemical test is shown in Table 1. Prepared steel specimens with dimension of 3 cm × 3 cm × 0.7 cm, were polished followed degreasing by acetone. In order to seal the edges and back sides of the steel panels, they were covered by a mixture of bees wax and colophony resin and an area of 1 cm^2 of each plate was exposed to the electrolytes.

2.2 NZF pigment extracts preparation

NZF pigments selected for this study were synthesized by sol-gel method. For this reason, ferric nitrate [$Fe(NO_3)_3.9H_2O$, Merck] and zinc nitrate [$Zn(NO_3)_2.6H_2O$, Merck] were separately dissolved in ethylene glycol ($C_2H_6O_2$, Merck). The two solutions were mixed together with the stoichiometric ratio to achieve zinc ferrite ($ZnFe_2O4$). The obtained solution was dried at 80 °C for 6 h, and then the calcinations step was carried out at three different temperatures of 500, 600, and 800 °C for 2 h with a heating rate of 10 °C/min, resulting three powders entitled α, β, and γ-NZF, respectively. The details of this method have been explained elsewhere[32-34].

Extraction of NZF pigments was proceeded as described by Pouget et al.[35]. In this step, 1 g of α, β, and γ-NZF pigments were added to 500 cc of 3.5 wt. % NaCl solution, stirred for 48 h, and incubated overnight. The solutions were then filtered to gain NZF pigment extract.

2.3 Characterization

EIS and Tafel polarization measurements were made using an electrochemical interface and impedance analyzer (Compact stat, Ivium, Netherlands). The electrochemical cell was including of the mild steel sample, Ag/AgCl electrode, and platinum electrodes as working, reference and counter electrodes, respectively. The tests were conducted as a function of immersion time, namely after 1, 4 and 44 h, to indicate how electrochemical parameters varied depending upon the immersion period. Each test accomplished using three replicate panels to ensure repeatability.

The impedance measurements were carried out using a sine wave of 20 mV amplitude peak to peak at the open circuit potential (OCP) in 3.5 wt. % NaCl solution. The frequency range was from 10 kHz down to 10 mHz. Ivium equivalent circuit evaluator software was utilized to calculate the EIS parameters and analyze the obtained spectra. The EIS parameters, including CPE (constant phase element), CPE_{dl} (constant phase element of double layer), CPE_f (constant phase element of film), R_s (solution resistance), Rct (charge transfer resistance), C_{dl} (double layer capacitance),$Y_{0,dl}$ (admittance of the CPE_{dl}), n_{dl} (exponent of the CPE_{dl}), R_f (film resistance), $Y_{0,f}$ (admittance of the CPE_f), n_f (exponent of the CPE_f), and C_f (film capacitance), were obtained from the equivalent circuit and impedance data[36]. The double layer and inhibitive film capacitance values could be calculated by Eq. 1.

$$C = (Y_0.R^{1-n})^{1/n} \quad (1)$$

Where Y_0 is the magnitude of admittance of the CPE ($S^n/\Omega.cm$) and n is the CPE exponent related to surface heterogeneity[37].

Tafel polarization tests were carried out with the scan rate of 1 mV/sec and potential range ±100 mV with respect to OCP in 3.5 wt.% NaCl solution. Powersuite software (Ametek, Princeton Applied Research, TN, USA) was used to calculate the Tafel parameters, such as corrosion current density (i_{corr}) and corrosion potential (E_{corr}). In addition, the anodic and cathodic β Tafel constants (b_a and b_c) were estimated via Tafel extrapolation technique. R_p (polarization resistance) were calculated via Eq. 2[38].

$$R_p = (b_a \times b_c)/[2.303 \times i_{corr} \times (b_a + b_c)] \quad (2)$$

Transmission electron microscopy (TEM, CM200 FEG, Philips, Netherlands) was used to compare the particles size and morphology of the as-synthesized nanoparticulates pigments.

Scanning electron microscopy (SEM) was operated to study morphology of the film formed on the surface after 44 h and was accomplished by SEM (1455 VP, LEO, Japan). The elemental and composition of the deposited compounds

Table 1. Composition of steel panels used for the electrochemical test

Elements	C	Si	Mn	Cr	Mo	Co	Cu	Nb	Fe
wt. %	0.190	0.288	1.390	0.026	0.018	0.388	0.297	0.334	balance

were studied by energy dispersive X-ray analysis (EDX, 50 KV, Horiba XGT 7200). EDX analysis was used in an area corresponded directly to the SEM imaging at least three areas were analyzed for the given depth of each sample. Elements chosen for analysis were based on the known chemical components of the NZF, NaCl solution, and steel panels.

The inductively coupled plasma-optical emission spectrometry (ICP-OES) was carried out by an equipment (Vista MPX, Varian Inc., Palo Alto, CA, USA). The test solutions containing α, β, and γ-NZF pigments were analyzed under two conditions; before immersion (intact solutions) and after 44 h of immersion (exposed solutions).

3. Results and Discussion

3.1. Microstructure Analysis of the as-synthesized pigments

Figure 1 shows the TEM images of the as-synthesized powder pigments, along with the particle size distributions. It is clear that the particle size of the pigments have a direct relation with calcining temperature. The α-NZF sample contains nanoparticles with a size distribution ranging from 5 to 30 nm and ~ 70% of the particles lie in the range of 10-15 nm. With an increase in the calcining temperature, the particle size distribution shifted to larger particle size. In case of β-NZF, more than 80% of the particles lie in the range of 10-20 nm, whereas the γ-NZF pigment contains particles that are dominantly in the range of 15-25 nm.

3.2. EIS measurements

Nyquist and Bode diagrams for carbon steel after 1, 4, and 44 h immersion in the blank solution (3.5 wt. % NaCl) and pigments containing solutions (α, β, and γ-NZF pigments in 3.5 wt. % NaCl solution) are shown in Figure 2. It can be seen that in α- and β-NZF pigments (see Figure 2 and 3), the increase in absolute values of impedance at low frequencies in Bode plots and the increase in the semicircle diameter in Nyquist plots confirm the higher protection obtained when immersion time is increased. In other words, when comparing 1 h, 4 h and 44 h immersion, an explicit decrease in phase angle can be seen. The mechanism of this phenomenon should be further explored by equivalent circuits fitting and microscopic investigation.

The electrical equivalent circuits used to fit the EIS results with typical fitting curves are shown in Figure 3 and the extracted EIS parameters are listed in Table 2. The suggested equivalent circuit has been previously reported for the epoxy coatings pigmented with zinc aluminum polyphosphate[1], inhibitive hybrid pigment based on zinc acetate-Cichorium intybus L leaves extract[39], and lithium zinc phosphate pigment[40]. The relationship between protection performance and pigment types may be related to adsorption enhancement of small NZF (Figure 1) on the mild steel surface. Whereas, in γ-NZF pigment (see Figure 2-4) the impedance magnitude at low frequencies in Bode plots and the semicircle diameter in Nyquist plots are declined during immersion time which may be on account of repulsion between big nanoparticulates (Figure 1) and probably desorption of nanoparticulates from metal surface resulting in diminution performance at final immersion time. The one simple peak in the Bode plot and one depressed capacitive loop in the Nyquist plot were observed for β- and α-NZF pigments, which are attributed to the presence of one time constant in the corrosion process relating to the electrical double layer existence in metal/solution interface (see Figure 3). However, in EIS diagrams of metal immersed in α-NZF pigment containing solution, there are two distinct peaks in the Bode plot and two overlapping semicircles in Nyquist plot. This is related to the presence of two time constants in the corrosion process (see Figure 3), which shows formation of an inhibitive film beside the electrical double layer existence on the metal/electrolyte interface. Deviation of the capacitive loop from a perfect semicircle could be attributed to surface heterogeneity[41].

From the fitting, it is clear that increasing the charge transfer resistance and decreasing the double layer capacitance in metals immersed in solutions containing nanoparticulates were occurred via nanopigment absorption enhancement and resultant double layer thickness increment during immersion periods. In other words, all three pigments led to lower double layer capacitance than the sample in pigment-free solution. This observation could be related to the quality and thickness of the as-deposited layer. By the time the protective film is built-up, it *generates a resistance* that slows down the corrosion rate[39,42]. On the other hand, the existence of the pigments has some remarkable effects for decreasing the admittance values. The lowest admittance could be observed in the case of α-NZF pigment. Comparisons between resulted data in Table 2 imply the better performance of α- than β- and subsequently γ-NZF. This result may be attributed to smaller particle size of α-NZF (see Figure 1) which can be adsorbed more easily compared to other nanoparticles on the mild steel surface. The application of these pigments leads to diminish the possible corrosive attack via formation of a protective film[43]. According to Table 2, R_{ct} values after 44 h are about 798 (Blank), 3475 (α-NZF), 935 (β-NZF), and 1491 (γ-NZF) $\Omega.cm^2$. Therefore, the α-NZF pigment is much more impressive in anticorrosion performance, due to the formation of a perfect protective film on the substrate during immersion period. This agrees well with recent sentences in the previous paragraph. In overall, the results of EIS (increase in the charge transfer resistance, and decrease in the admittance and capacitance values due to the application of α-NZF pigment) showed that in the presence of the as-synthesized pigments, especially α-NZF sample, the inhibition performance was improved significantly relative to metal immersed in blank solution. This may be related

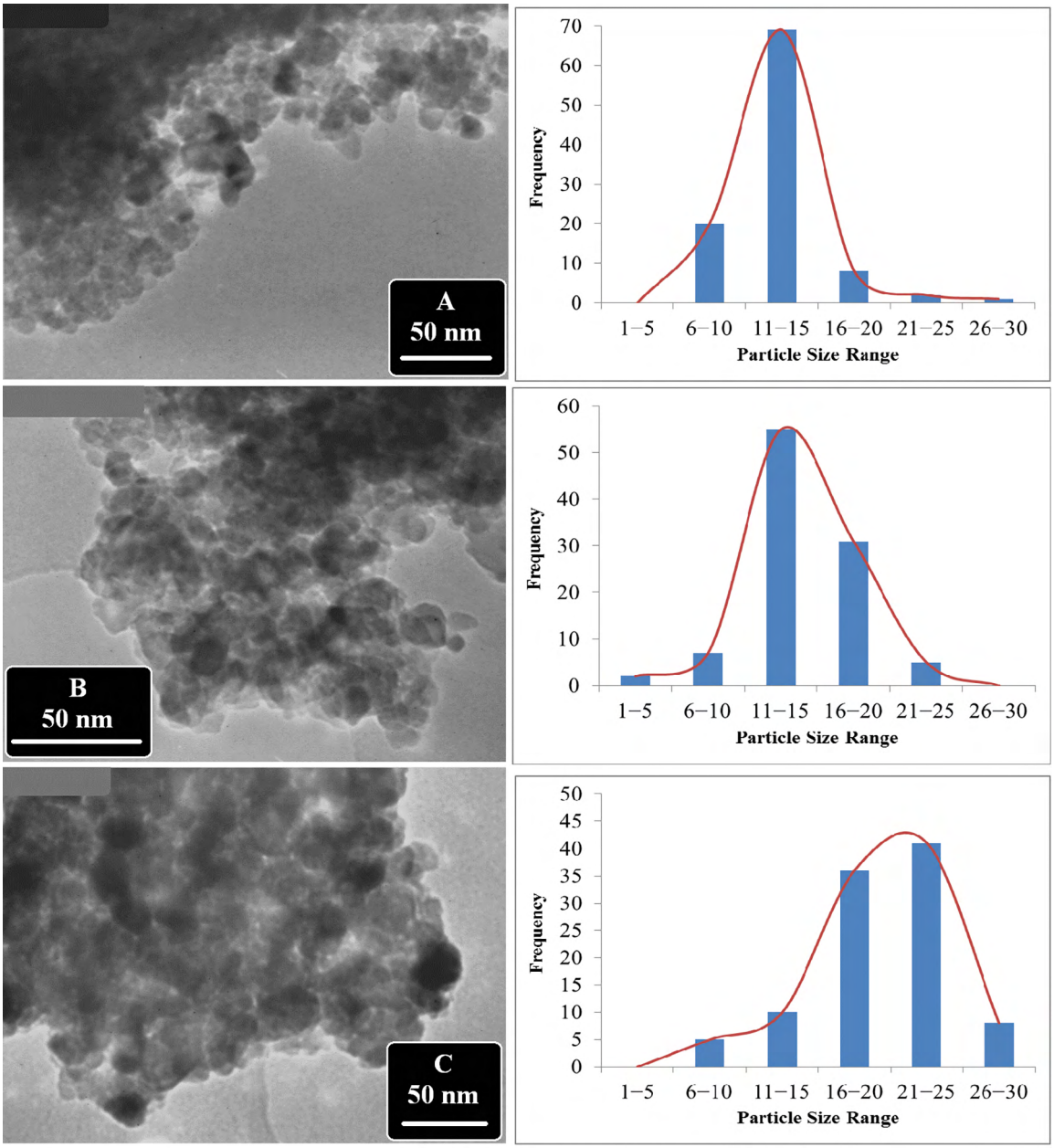

Figure 1. TEM images and histograms of size distribution of the synthesized pigments (A) α-NZF, (B) β-NZ,F and (C) γ-NZF.

to replacement of nanopigments with water molecules[44] and increasing the thickness of electrical double layer and inhibitor film due to NZF adsorption increment on mild steel surface during immersion time[39].

3.3. Tafel polarization measurements

Figure 4 compares the polarization results for the samples immersed in the test solutions after 1, 4 and 44 h. The resulted data of Tafel polarization measurements are listed in Table 3. Using Tafel extrapolation, i_{corr} and R_p were determined which are presented in Figure 5.

E_{corr} becomes more negative and R_p of all samples was decreased during immersion time. In addition, i_{corr} for steel immersed in α-NZF containing solution was slightly increased, whereas for β- and γ-NZF contained solutions diminution of i_{corr} was observed with exposing time. On the other hand, all three pigments led to lower R_p than the sample in pigment-free solution. With similarity of EIS results, α-NZF have better proficiency relative to other nanopigments (β-NZF and γ-NZF) and subsequently nanopigments (α-, β- and γ-NZF) contained solutions relative to the blank one, as the higher R_p, nobler E_{corr} and lesser i_{corr} was attained with

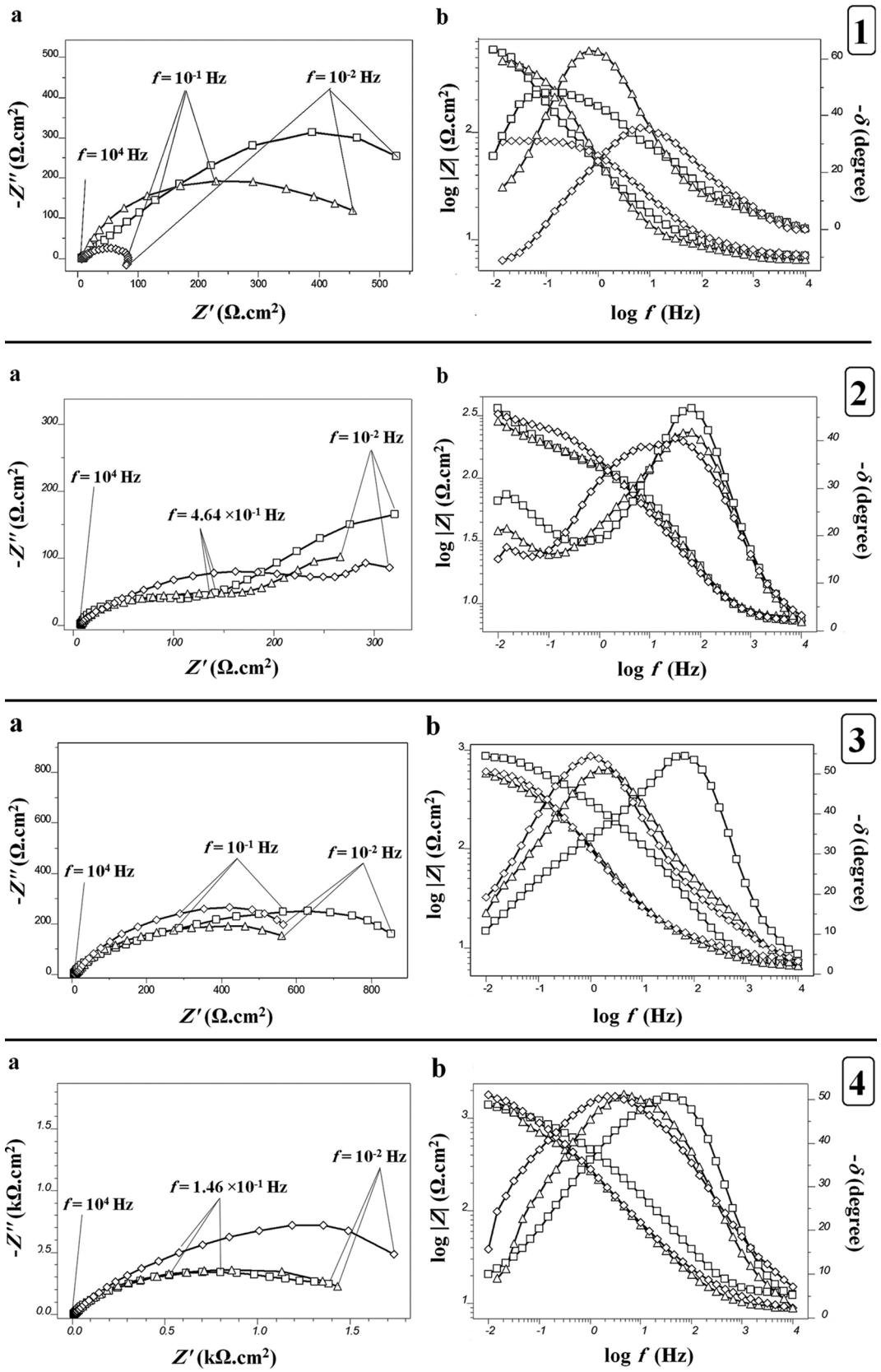

Figure 2. Nyquist and Bode diagrams for the mild steel after 1(□), 4 (Δ) and 44 h (◊) immersion in the test solutions. (1) the blank solution. (2) α-NZF containing solution. (3) β-NZF containing solution. (4) γ-NZF containing solution.

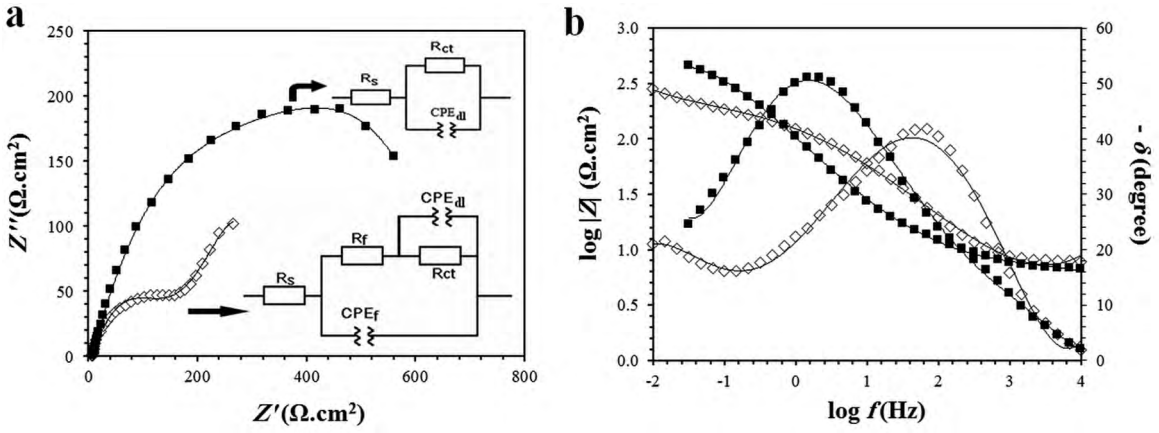

Figure 3. Equivalent electrical circuits used to fit the EIS results.

Table 2. Variation of electrochemical parameters of mild steel after 1,4 and 44 h immersion in 3.5 wt. % NaCl solutions.

Test solution	Immersion time (h)	R_{ct} ($\Omega.cm^2$)	$Y_{0,dl}$ ($\mu s^n.\Omega^{-1}.cm^{-2}$)	n_{dl}	C_{dl} ($\mu F/cm^2$)	R_f ($\Omega.cm^2$)	$Y_{0,f}$ ($\mu s^n.\Omega^{-1}.cm^{-2}$)	n_f	C_f ($\mu F/cm^2$)
Blank	1	85.5	125.81	0.66	12.6	–	–	–	–
	4	516.3	105.03	0.72	56.4	–	–	–	–
	44	798.5	267.84	0.61	99.23	–	–	–	–
α-NZF containing	1	534	0.11	0.37	5.26 E-9	66.3	0.42	0.78	7.93
	4	1822	2.75	0.35	1.46 E-4	83.6	0.43	0.74	5.89
	44	3475	4.01	0.37	2.77 E-3	69.3	0.66	0.86	0.28
β-NZF containing	1	783	254.20	0.72	135.7	–	–	–	–
	4	676	148.70	0.67	47.9	–	–	–	–
	44	935	20.01	0.71	3.94	–	–	–	–
γ-NZF containing	1	2412	20.60	0.63	3.37	–	–	–	–
	4	1789	25.50	0.65	4.82	–	–	–	–
	44	1491	26.40	0.64	4.28	–	–	–	–

α-NZF pigment. Comparison of the results shows that the inhibition performance of the samples is as below:

$$\alpha\text{-NZF} >> \beta\text{-NZF} > \gamma\text{-NZF} > \text{blank solution}$$

The partly changes of both anodic and cathodic Tafel slopes and also i_{corr} during immersion (on contrary of the blank solution) was indicated these nanoparticulates have mixed behavior in NaCl solution, since it was influenced on both anodic and cathodic reactions verifying the positive effect on corrosion rate decrement of mild steel specimens exposed to corrosive 3.5 wt. % NaCl solution. This statement is supported by results of R_p calculation. This parameter is influenced by b_a, b_c, and i_{corr}.

Another significant result that comes from Figure 5 is that it takes time for the corrosion inhibitor to kick in. In other word, the difference in i_{corr} exceeds one order of magnitude after 44 h. Therefore, this type of pigments can be classified as sluggish corrosion inhibitor. This concept has been considered in the previous works[45,46].

3.4. Surface analysis (SEM/EDS)

The SEM micrographs are represented in Figure 6. Comparing to the samples immersed in the blank solution, it is obvious that a film is formed on the mild steel surface after exposure to NZF extracts. The zinc content in the surface film analyzed by EDS shows the presence of 13.9%, 12.9%, 5.1% and 0.0% (w/w) on samples exposed to the α-NZF, β-NZF, γ-NZF, and the blank solution, respectively. Evidence provided by SEM results confirmed the inferences made in sections 3.1 and 3.2 relating to film formation. Moreover, EDS results showed the rare presence of ingredients as, Al, Si, Cl, K, Na, and Mn in the precipitated layer on steel substrates. In addition, Na percentage on the samples' surface is more than Cl that have a connection with creation of insoluble anionic complex. Actually, incorporation of NZF compounds into the primer is thought to be very applicable because developed deposition might promote primer adhesion to substrate and also prevent corrosion by their inhibitive performance. Presence of zinc element in EDS is related to deposition of insoluble complex of zinc with steel surface and corrosion products.

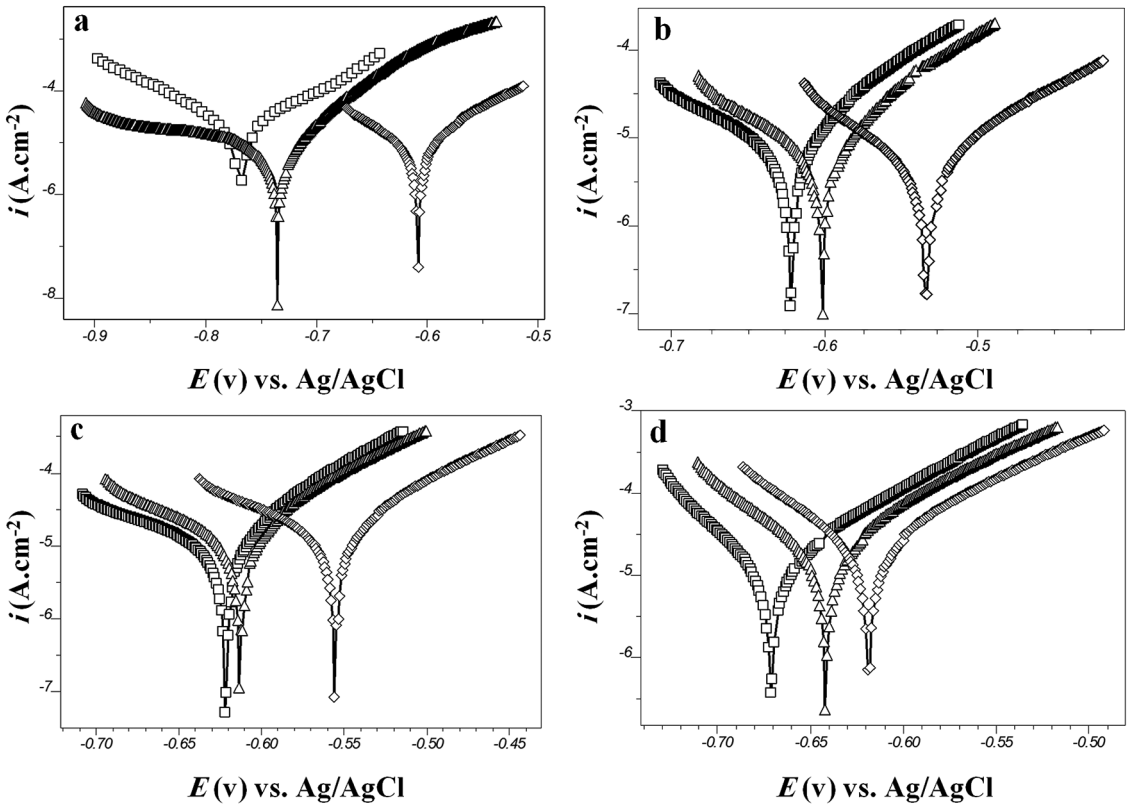

Figure 4. Polarization curves of steel samples after 1 (◊), 4 (Δ), and 44 h (□) immersion in 3.5 wt. % NaCl solution containing: (a) nothing, (b) α-NZF, (c) β-NZ,F and (d) γ-NZF.

Table 3. Variation of corrosion kinetic parameters of steel samples after 1, 4, and 44 h immersion in 3.5 wt. % NaCl solution without (blank) and with α–, β–, and γ–NZF extract.

Test solution	Immersion time (h)	b_a (V/dec)	b_c (V/dec)	E_{corr} (V vs.Ag/AgCl)	i_{corr} (A/cm^2)	R_p (Ω.cm^2)
Blank	1	0.075	0.070	-0.6152	6.917 E-5	227
	4	0.076	0.042	-0.7409	7.109 E-5	165
	44	0.096	0.015	-0.7472	3.941 E-5	143
α–NZF containing	1	0.100	0.083	-0.5427	4.618 E-6	4265
	4	0.076	0.100	-0.6074	6.770 E-6	2770
	44	0.077	0.110	-0.6296	7.187 E-6	2737
β–NZF containing	1	0.082	0.104	-0.5626	1.366 E-5	1457
	4	0.078	0.102	-0.6208	1.268 E-5	1514
	44	0.070	0.125	-0.6291	0.985 E-5	1978
γ–NZF containing	1	0.090	0.062	-0.6263	2.126 E-5	750
	4	0.084	0.060	-0.6505	1.953 E-5	778
	44	0.080	0.047	-0.6782	1.182 E-5	1088

3.5. ICP-OES measurements

Table 4 shows some characteristics of the NZF pigment extracts before and after 44 h immersion of the mild steel samples. According to the Table 3, corrosion of mild steel samples during immersion time in solutions and creation of alkali products can be reason of little increment of pH values[47]. Among of pH values, least increase is related to α-NZF extract that means least corrosion process occurred and subsequently least hydroxyl groups created.

According to the ICP-OES results, the proportion and percentages of iron in NZF pigments were 127.53 ppm and 13.94 wt. %, respectively. These values for zinc in

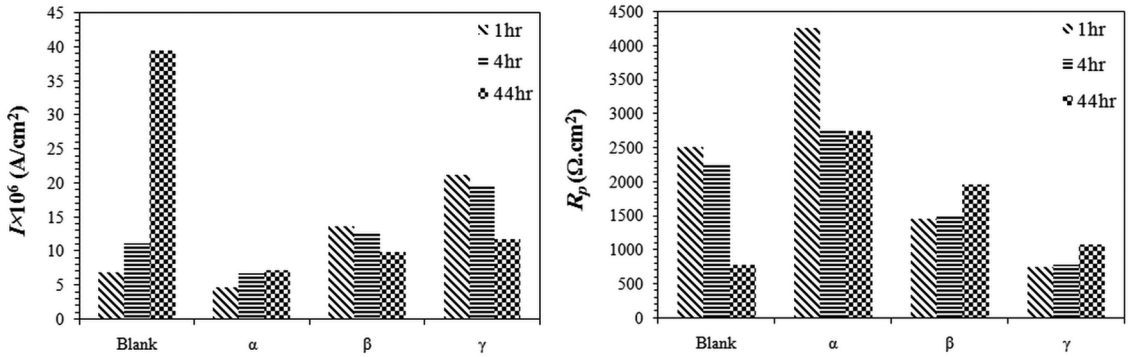

Figure 5. The corrosion current density (left) and polarization resistance (right) of the samples immersed in the test solutions.

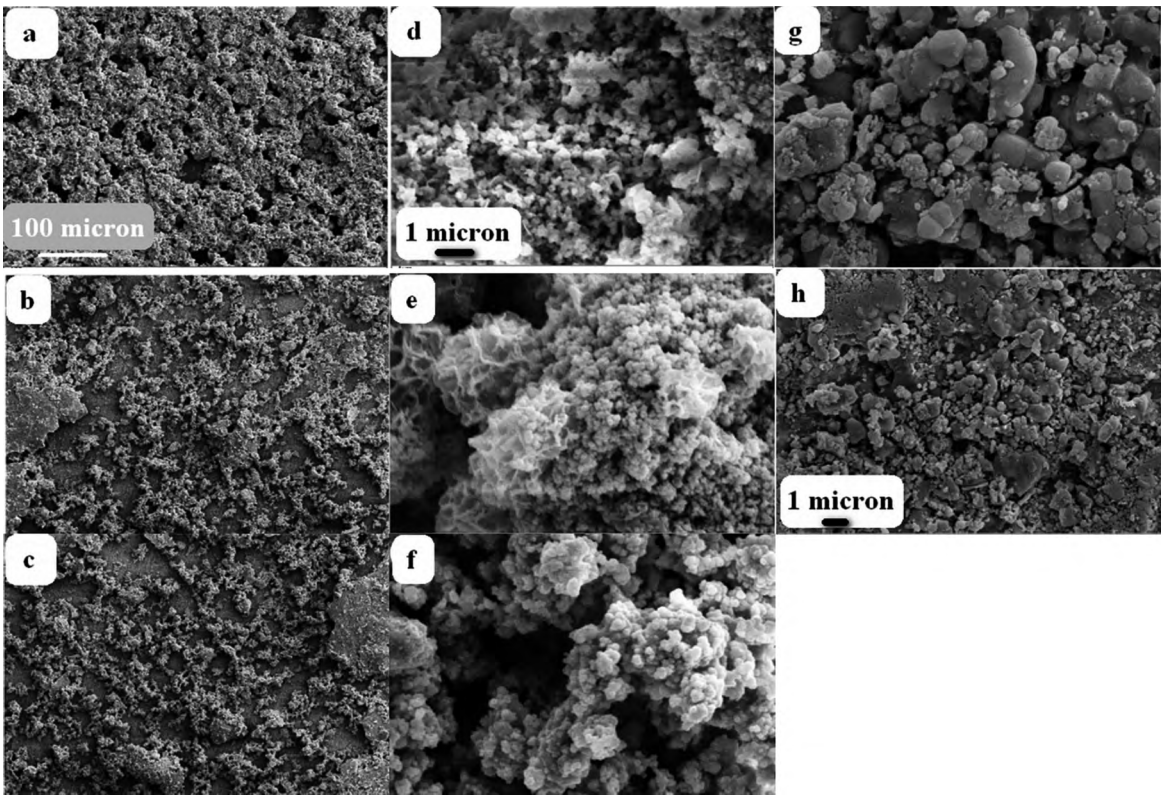

Figure 6. SEM Morphology of the precipitated layers on the surface of samples in α-NZF (a & d), β-NZF (b & e), γ-NZF (c & f) and the blank solution (g & h) after 44 h immersion.

Table 4. Some characteristics of the test solutions contain α–, β–, and γ–NZF for intact solutions, before immersion of the mild steel samples and for exposed solutions, after 44 h immersion.

Time	Characteristic	Pigment extracts		
		α–NZF	β–NZF	γ–NZF
before immersion (Intact solution)	pH	7.48±0.03	7.35±0.12	7.26±0.08
	Fe concentration (ppm)	0.059711	0.067613	1.3388
	Zn concentration (ppm)	10.095	10.639	7.1138
44 h immersion (Exposed solution)	pH	7.58±0.23	7.54±0.09	7.38±0.28
	Fe concentration (ppm)	0.053138	0.051585	0.057794
	Zn concentration (ppm)	8.4892	7.3954	6.8327

NZF pigments are 54.593 ppm and 5.97 wt. %. Moreover, according to the content of zinc and iron elements in solution before and after 44 h immersion of steel samples, there is obvious decrease relate to segregation from solution phase and deposition on the steel samples. Furthermore, results of SEM/EDS approved presence of these elements on steel samples.

4. Conclusions

This study aimed to evaluate the corrosion inhibition performance of nanoparticulates zinc ferrite pigments with different particle sizes. The performance of steel samples immersed in 3.5 wt. % NaCl aqueous solution-containing NZF pigments with different particle sizes, were investigated by using electrochemical tests such as electrochemical impedance spectroscopy and Tafel polarization as well as surface analysis. Based on the results of SEM and EDS, presence of a precipitated layer on the surface was confirmed when steel sample was immersed into the solution-containing NZF pigments. The joint use of the SEM, electrochemical impedance and Tafel polarization gave information on the several aspects of the system properties, corrosion rates and morphology. EIS results in total agreement with results of polarization test demonstrated superiority of NZF as an anti-corrosion pigment. In the case of samples exposed to α-NZF extract, the higher resistance and lower double layer capacitance extracted from impedance spectra as well as lower current density from polarization measurement results might be attributed to precipitation of an inhibitive layer on the surface. This was also supported by SEM/EDS results.

5. References

1. Naderi R, Attar MM. Electrochemical study of protective behavior of organic coating pigmented with zinc aluminum polyphosphate as a modified zinc phosphate at different pigment volume concentrations. *Progress in Organic Coatings*. 2009;66(3):314-320. DOI: 10.1016/j.porgcoat.2009.08.009

2. Lin BL, Lu JT, Kong G. Effect of molybdate post-sealing on the corrosion resistance of zinc phosphate coatings on hot-dip galvanized steel. *Corrosion Science*. 2008;50(4):962-967. DOI: 10.1016/j.corsci.2007.12.002

3. Bastos AC, Ferreira MGS, Simões AM. Comparative electrochemical studies of zinc chromate and zinc phosphate as corrosion inhibitors for zinc. *Progress in Organic Coatings*. 2005;52(4):339-350. DOI: 10.1016/j.porgcoat.2004.09.009

4. Chang YT, Wen NT, Chen WK, Ger MD, Pan GT, Yang TCK. The effects of immersion time on morphology and electrochemical properties of the Cr(III)-based conversion coatings on zinc coated steel surface. *Corrosion Science*. 2008;50(12):3494-3499. DOI: 10.1016/j.corsci.2008.08.051

5. Naderi R, Attar MM. Electrochemical assessing corrosion inhibiting effects of zinc aluminum polyphosphate (ZAPP) as a modified zinc phosphate pigment. *Electrochimica Acta*. 2008;53(18):5692-5696. DOI: 10.1016/j.electacta.2008.03.029

6. Bastos AC, Ferreira MG, Simões AM. Corrosion inhibition by chromate and phosphate extracts for iron substrates studied by EIS and SVET. *Corrosion Science*. 2006;48(6):1500-1512. DOI: 10.1016/j.corsci.2005.05.021

7. Kalendová A, Kalenda P, Veselý D. Comparison of the efficiency of inorganic nonmetal pigments with zinc powder in anticorrosion paints. *Progress in Organic Coatings*. 2006;57(1):1-10. DOI: 10.1016/j.porgcoat.2006.05.015

8. Yu X, Wang J, Zhang M, Yang L, Li J, Yang P, et al. Synthesis, characterization and anticorrosion performance of molybdate pillared hydrotalcite/*in situ* created ZnO composite as pigment for Mg-Li alloy protection. *Surface and Coatings Technology*. 2008;203(3-4):250-255. DOI: 10.1016/j.surfcoat.2008.08.074

9. Havlík J, Kalendová A, Veselý D. Electrochemical, chemical and barrier action of zinc dust/anticorrosive pigments containing coatings. *Journal of Physics and Chemistry of Solids*. 2007;68(5-6):1101-1105. DOI: 10.1016/j.jpcs.2006.11.016

10. Carboneras M, Hernández LS, del Valle JA, García-Alonso MC, Escudero ML (2010) Corrosion protection of different environmentally friendly coatings on powder metallurgy magnesium. *Journal of Alloys and Compounds*. 2010;496(1-2):442-448. DOI: 10.1016/j.jallcom.2010.02.043

11. Sinko J. Challenges of chromate inhibitor pigments replacement in organic coatings. *Progress in Organic Coatings*. 2001;42(3-4):267-282. DOI: 10.1016/S0300-9440(01)00202-8

12. Buxbaum G, ed. *Industrial Inorganic Pigments*. Weinheim: Wiley-VCH; 1998.

13. Fragata F, de la Fuente D, Almeida E, Santos D, Morcillo M. Solventborne paint systems on carbon steel and hot-dip galvanised steel for a wide range of atmospheric exposures. *Journal of Coatings Technology Research*. 2007;4(1):75-87.

14. Thorn A, Adams A, Gichuhi T, Novelli W, Hallox M. Improved corrosion control through nontoxic corrosion inhibitor synergies. *Journal of Coatings Technology*. 2006;3(5):24-30.

15. Hernández M, Genescá J, Uruchurtu J, Galliano F, Landolt D. Effect of an inhibitive pigment zinc-aluminum-phosphate (ZAP) on the corrosion mechanisms of steel in waterborne coatings. *Progress in Organic Coatings*. 2006;56(2-3):199-206. DOI: 10.1016/j.porgcoat.2006.05.001

16. Galliano F, Landolt D. Evaluation of corrosion protection properties of additives for waterborne epoxy coatings on steel. *Progress in Organic Coatings*. 2002;44(3):217-225. DOI: 10.1016/S0300-9440(02)00016-4

17. Beiro M, Collazo A, Izquierdo M, Nóvoa XR, Pérez C. Characterisation of barrier properties of organic paints: the zinc phosphate effectiveness. *Progress in Organic Coatings*. 2003;46(2):97-106. DOI: 10.1016/S0300-9440(02)00216-3

18. Kalenda P, Kalendová A, Veselý D. Properties of anticorrosion pigments depending on their chemical composition and PVC value. *Pigment & Resin Technology*. 2009;35(4):188-199. DOI: 10.1108/03699420610677181

19. Bethencourt M, Botana FJ, Marcos M, Osuna RM, Sánchez-Amaya JM. Inhibitor properties of "green" pigments for paints. *Progress in Organic Coatings*. 2003;46(4):280-287. DOI: 10.1016/S0300-9440(03)00013-4

20. Shao Y, Jia C, Meng G, Zhang T, Wang F. The role of a zinc phosphate pigment in the corrosion of scratched epoxy-coated steel. *Corrosion Science*. 2009;51(2):371-379. DOI: 10.1016/j.corsci.2008.11.015

21. Romagnoli R, Vetere VF. Non-Pollutant Corrosion Inhihitive Pigments: Zinc-Phosphate, A Review. *Corrosion Reviews*. 1995;13(1):45-64. DOI: 10.1515/CORRREV.1995.13.1.45

22. Blustein G, del Amo B, Romagnoli R. The influence of the solubility of zinc phosphate pigments on their anticorrosive behaviour. *Pigment & Resin Technology*. 2000;29(2):100-107. DOI: 10.1108/03699420010319148

23. del Amo B, Romagnoli R, Deyá C, González JA. High performance water-based paints with non-toxic anticorrosive pigments. *Progress in Organic Coatings*. 2002;45(4):389-397. DOI: 10.1016/S0300-9440(02)00125-X

24. Romagnoli R, Deyá MC, del Amo B. The mechanism of the anticorrosive action of calcium-exchanged silica. *Surface Coatings International Part B: Coatings Transactions*. 2003;86(2):135-141. DOI: 10.1007/bf02699625

25. Kalendová A. Alkalising and neutralising effects of anticorrosive pigments containing Zn, Mg, Ca, and Sr cations. *Progress in Organic Coatings*. 2000;38(3-4):199-206. DOI: 10.1016/S0300-9440(00)00103-X

26. Abd El-Ghaffar MA, Ahmed NM, Youssef EA. A method for preparation and application of micronized ferrite pigments in anticorrosive solvent-based paints. *Journal of Coatings Technology and Research*. 2010;7(6):703-713. DOI: 10.1007/s11998-009-9229-6

27. Li Y, Yi R, Yan A, Deng L, Zhou K, Liu X. Facile synthesis and properties of $ZnFe_2O_4$ and $ZnFe_2O_4$/polypyrrole core-shell nanoparticles. *Solid State Sciences*. 2009;11(8):1319-1324. DOI: 10.1016/j.solidstatesciences.2009.04.014

28. Narasimhan BRV, Kumar S, Sankara Narayanan TSN. Synthesis of manganese zinc ferrite using ferrous pickle liquor and pyrolusite ore. *Environmental Chemistry Letters*. 2011;9(2):243-250. DOI: 10.1007/s10311-009-0272-4

29. Masala O, Hoffman D, Sundaram N, Page K, Proffen T, Lawes G, et al. Preparation of magnetic spinel ferrite core/shell nanoparticles: Soft ferrites on hard ferrites and vice versa. *Solid State Sciences*. 2006;8(9):1015-1022. DOI: 10.1016/j.solidstatesciences.2006.04.014

30. Tanaka K, Nakashima S, Fujita K, Hirao K. Large Faraday effect in a short wavelength range for disordered zinc ferrite thin films. *Journal of Applied Physics*. 2006;99(10):106103. DOI: 10.1063/1.2199727

31. Cayton RH, Sawitowski T. The impact of Nano-materials on coating technologies. In: *Technical Proceedings of the 2005 NSTI Nanotechnology Conference and Trade Show*. Volume 2. *Nano Composites. Chapter 2*. 2005 May 8-12; Anaheim, CA, USA. p. 83-85.

32. Ehsani M, Borsi H, Gockenbach E, Morshedian J, Bakhshandeh GR. An investigation of dynamic mechanical, thermal, and electrical properties of housing materials for outdoor polymeric insulators. *European Polymer Journal*. 2004;40(11):2495-2503. DOI: 10.1016/j.eurpolymj.2004.03.014

33. Iqbal F, Mutalib MIA, Shaharun MS, khan M, Abdullah B. Synthesis of $ZnFe_2O_4$ Using sol-gel Method: Effect of Different Calcination Parameters. *Procedia Engineering*. 2016;148:787-794. DOI: 10.1016/j.proeng.2016.06.563

34. Pradeep A, Priyadharsini P, Chandrasekaran G. Structural, magnetic and electrical properties of nanocrystalline zinc ferrite. *Journal of Alloys and Compounds*. 2011;509(9):3917-3923. DOI: 10.1016/j.jallcom.2010.12.168

35. Pouget MP, Legeune B, Vennat B, Pourrat A. Extraction, analysis and study of the stability of *Hibiscus* anthocyanins. *Lebensmittel-Wiissenschaft & Technologie*. 1990;23(2):103-105.

36. Bentiss F, Jama C, Mernari B, Attari HE, Kadi LE, Lebrini M, et al. Corrosion control of mild steel using 3,5-bis(4-methoxyphenyl)-4-amino-1,2,4-triazole in normal hydrochloric acid medium. *Corrosion Science*. 2009;51(8):1628-1635. DOI: 10.1016/j.corsci.2009.04.009

37. Motamedi M, Tehrani-Bagha AR, Mahdavian M. Effect of aging time on corrosion inhibition of cationic surfactant on mild steel in sulfamic acid cleaning solution. *Corrosion Science*. 2013;70:46-54. DOI: 10.1016/j.corsci.2013.01.007

38. Chaker V. *Corrosion Forms and Control for Infrastructure*. ASTM 1137. Philadelphia: ASTM; 1992.

39. Sanaei Z, Shahrabi T, Ramezanzadeh B. Synthesis and characterization of an effective green corrosion inhibitive hybrid pigment based on zinc acetate-Cichorium intybus L leaves extract (ZnA-CIL.L): Electrochemical investigations on the synergistic corrosion inhibition of mild steel in aqueous chloride solutions. *Dyes and Pigments*. 2017;139:218-232. DOI: 10.1016/j.dyepig.2016.12.002

40. Alibakhshi E, Ghasemi E, Mahdavian M. The influence of surface modification of lithium zinc phosphate pigment on corrosion inhibition of mild steel and adhesion strength of epoxy coating. *Journal of Sol-Gel Science and Technology*. 2014;72(2):359-368. DOI: 10.1007/s10971-014-3441-2

41. Motamedi M, Tehrani-Bagha AR, Mahdavian M. A comparative study on the electrochemical behavior of mild steel in sulfamic acid solution in the presence of monomeric and gemini surfactants. *Electrochimica Acta*. 2011;58:488-496. DOI: 10.1016/j.electacta.2011.09.079

42. Alibakhshi E, Ghasemi E, Mahdavian M. A Comparison Study on Corrosion Behavior of Zinc Phosphate and Potassium Zinc Phosphate Anticorrosive Pigments. *Progress in Color, Colorants and Coatings*. 2012;5(2):91-99.

43. Bojinov M, Betova I, Raicheff R. Kinetics of formation and properties of a barrier oxide film on molybdenum. *Journal of Electroanalytical Chemistry*. 1996;411(1-2):37-42. DOI: 10.1016/0022-0728(96)04591-3

44. Bella F, Gerbaldi C, Barolo C, Grätzel M. Aqueous dye-sensitized solar cells. *Chemical Society Reviews*. 2015;44(11):3431-3473. DOI: 10.1039/C4CS00456F

45. Li J, Hurley B, Buchheit R. The Effect of $CeCl_3$ as an Inhibitor on the Localized Corrosion of AA2024-T3 as a Function of Temperature. *Journal of The Electrochemical Society*. 2016;163(14):C845-C852. DOI: 10.1149/2.0561614jes

46. Yousefi A, Javadian S, Neshati J. A New Approach to Study the Synergistic Inhibition Effect of Cationic and Anionic Surfactants on the Corrosion of Mild Steel in HCl Solution. *Industrial & Engineering Chemistry Research*. 2014;53(13):5475-5489. DOI: 10.1021/ie402547m

47. Mendez C, Singer M, Comacho A, Nesic S, Hernandez S, Sun Y, et al. Effect of Acetic Acid, pH and MEG on the CO_2 Top of the Line Corrosion. In: *NACE Conference CORROSION 2005*; 2005 Apr 3-7; Houston, TX, USA.